

Knockdown of long non-coding RNA VIM-AS1 inhibits glioma cell proliferation and migration, and increases the cell apoptosis *via* modulation of WEE1 targeted by miR-105-5p

S.-T. SUO, P. GONG, X.-J. PENG, D. NIU, Y.-T. GUO

Neurosurgery Department, Shangluo Central Hospital, Shangluo City, China

Abstract. – **OBJECTIVE:** Glioma including glioblastoma is the main type of primary brain tumors worldwide. LncRNAs have participated in glioma formation. This study aims to investigate the underlying mechanism for VIM-AS1/miR-105-5p/WEE1 signaling in glioma.

PATIENTS AND METHODS: The clinical tumors and adjacent tissues were collected from 24 patients with glioma in the Shang Luo Central Hospital. Then, the clinical samples were subjected to hematoxylin-eosin staining (H&E). VIM-AS1, miR-105-5p, and WEE1 levels were measured using real-time PCR. The protein levels of WEE1, Cyclin A1, PCNA, N-cadherin, Vimentin, and Bcl-2, E-cadherin, and Bax were analyzed using Western blot. The overall survival of glioma patients was evaluated using the Kaplan-Meier analysis. The interaction between VIM-AS1 and miR-105-5p was determined using RIP assay and Dual-Luciferase reporter assay, and the binding between miR-105-5p and WEE1 was also detected by Dual-Luciferase reporter assay. Cell proliferation, colony formation, cell cycle, apoptosis, and migration were confirmed using CCK-8, colony formation assay, flow cytometry, and transwell assay, respectively.

RESULTS: VIM-AS1 was elevated in cancer tissues, and high level of VIM-AS1 was positively correlated with poor overall survival. Then, VIM-AS1 could bind to and downregulate miR-105-5p. Furthermore, the knockdown of VIM-AS1 significantly suppressed tumor growth *in vivo*. The knockdown of VIM-AS1/overexpression of miR-105-5p inhibited glioma cell growth, colony formation, and migration, and enhanced the cell apoptosis by inhibiting expression of Cyclin A1, PCNA, Vimentin, N-cadherin, and Bcl-2, and by increasing the expression of Bax and E-cadherin. Interestingly, the overexpression of VIM-AS1 reversed the tumor-suppressing role of miR-105-5p in glioma cells. Besides, the expression of WEE1 was synergistically regulated by VIM-AS1 and miR-105-5p. Consequently, VIM-AS1 promoted glioma progression via upregulating WEE1 or downregulating miR-105-5p.

CONCLUSIONS: VIM-AS1/miR-105-5p/WEE1 signaling may be a promising target for glioma treatment.

Key Words:

VIM-AS1, MiR-105-5p, WEE1, Glioma, Xenografts.

Introduction

Glioma has been listed as the most commonly occurring kind of cerebral cancers or primary brain tumors in China, as well as in Europe and the United States^{1,2}. Glioblastoma (World Health Organization, grade IV), as the leading type of primary malignant brain tumor, accounts for eighty percent of patients every year³. The surgical resection, radiotherapy, and chemotherapy are usually prepared for the treatment of glioblastoma⁴. Unfortunately, the five-year survival rate of glioblastoma patients is about 9.8% in adults who are subjected to chemotherapy and radiotherapy³. In recent years, targeted therapy has been studied and used for its specificity and efficacy. Thus, it has become a hot topic in glioblastoma treatment⁴, and molecular mechanisms of gliomas are required to be investigated in detail^{5,6}. Consequently, it is beneficial for the treatment of patients with glioblastoma to obtain a better investigation of molecular mechanisms underlying glioma progression.

Long noncoding RNAs (lncRNAs), as oncogenic regulators or tumor suppressors, have afforded to both initiation and progression of many types of cancers, including gliomas⁷⁻¹¹. lncRNAs are often implicated in the transcriptional and post-transcriptional regulation of gene regulation¹². At the post-transcriptional level, lncRNAs usually serve as competing endogenous RNAs or molecular sponge of microRNAs (miRNAs) resulting in suppression of miRNAs on its downstream target mRNAs¹³. Of note, homeobox transcript antisense RNA (HOTAIR) promotes the malig-

nant biological functions of glioma cells through miR-326/fibroblast growth factor 1 (FGF1) axis¹⁴. The suppression of nuclear paraspeckle assembly transcript 1 (NEAT1) represses glioma cell migration and invasion by modulating the expression of miR-132-targeted sex-determining region Y-box transcription factor 2 (SOX2)¹⁵. Inhibition of SRY-box transcription factor 2 overlapping transcript (SOX2OT) suppresses the malignant effects of glioblastoma stem cells by increasing the levels of both miR-194-5p and miR-122¹⁰. Tumor protein 73 antisense RNA 1 (TP73-AS1) enhances glioma proliferation and invasion by regulating miR-142/HMGB1 signaling¹⁶. Colorectal neoplasia differentially expressed (CRNDE) facilitates glioma cell proliferation and invasion, while inhibited the cell apoptosis by attenuating miR-384/piwi-like RNA-mediated gene silencing 4 (PIWIL4)/signal transducer and activator of transcription 3 (STAT3) axis¹⁷. Imprinted maternally expressed transcript (H19) promotes glioblastoma cell invasion, angiogenesis, and tube formation by upregulating of the miR-29a-controlled vasohibin 2 (VASH2) expression¹⁸. X inactive specific transcript (XIST) enhances glioma tumorigenicity and angiogenesis by functioning as a sponge of miR-429¹⁹. Growth-arrest specific 5 (GAS5) suppresses glioma stem cell proliferation, migration, and invasion by forming GAS5/miR-196a-5p/forkhead box O1 (FOXO1) feedback loop²⁰. Metastasis associated lung adenocarcinoma transcript 1 (MALAT1) suppresses the invasion and proliferation of glioma cells by inhibiting miR-155 expression²¹. Vimentin antisense RNA 1 (VIM-AS1), a 1.8-kb noncoding RNA, positively modulates Vimentin expression²². VIM-AS1 promotes progression and metastasis of colorectal cancer by inducing EMT²³. However, the clinical functions of VIM-AS1 in glioma development remain unclear.

To explore the potential mechanism of VIM-AS1 in glioma development, we predicted that VIM-AS1 may directly bind to miR-105-5p on STARBASE database. As reported, miR-105-5p suppresses the proliferation of glioma cells by targeting sex-determining region Y-box 9 (SOX9)²⁴, and it inhibits metastasis of triple-negative breast cancer²⁵. Additionally, we predicted that miR-105-5p may bind to 3'UTR of Weel-like protein kinase (WEE1) using the STARBASE tool. WEE1 always serves as an oncogene in cancers, including gliomas²⁶⁻²⁸, and it has developed chemical inhibitors, such as Adavosertib-1775 (AZD-1775 or MK-1775), to target WEE1 resulting in suppression of

WEE1-mediated cancers²⁹⁻³³, suggesting that the inhibition of WEE1 expression would inhibit glioma cell proliferation, invasion, and metastasis.

In this study, high expression of VIM-AS1 represented an overall survival of glioma patients, indicating that it worked as an oncogene in glioma development. We observed that the VIM-AS1/miR-105-5p/WEE1 signaling was involved in glioma formation *in vitro* and *in vivo*. Taken together, VIM-AS1, miR-105-5p, and WEE1 may be listed as the promising therapeutic targets of glioma treatment.

Patients and Methods

Clinical Patients' Samples Collection

The clinical tumors and adjacent tissues were collected from 24 patients with glioma in Shang Luo Central Hospital (Shang Luo, Shan Xi, China). The clinical processes were approved by the Ethics Committee of Shang Luo Central Hospital (SLCH 2006-0018). No patients had administered local or systemic treatment before surgery. Then, the collected clinical samples were immediately frozen in liquid nitrogen.

Hematoxylin-Eosin Staining

The clinical samples were firstly fixed in 4% paraformaldehyde (Sigma-Aldrich, Shanghai, China). Next, these samples were subjected to paraffin blocks, section, and hematoxylin-eosin staining (H&E; Beyotime, Shanghai, China) conducted as previously described¹.

Cell Culture and Cell Transfection

These cell lines (HM, U87, U251, T98G, and LN-229) (American Type Culture Collection, Manassas, VA, USA) were kept in Dulbecco's Modified Eagle's Medium (DMEM) basic media (HyClone, Logan, UT, USA), and then, they were maintained in a 37°C humidified incubator with 5% CO₂. All the above media were prepared with 10% fetal bovine serum (FBS; Thermo Fisher Scientific, Waltham, MA, USA), and 100 µg/mL streptomycin, and 100 U/mL penicillin (HyClone, Logan, UT, USA). All the other cell culture materials were bought from HyClone (Logan, UT, USA).

All used siRNAs were purchased from GenePharma (Shanghai, China). VIM-AS1 sequences were downloaded from UCSC (ENST00000605833.1), and WEE1 sequences were downloaded from National Coalition Building Institute (NCBI) (mRNA ID: NM_003390.4). The siRNAs or plasmids were

transfected to cancer cell lines with Lipofectamine 3000 (Thermo Fisher Scientific, Waltham, MA, USA). Si-VIM-AS1#1: UUA AAU UUC AAA AUG UGG G, si-VIM-AS1#2: AUU AAA UUU CAA AAU GTG G, si-VIM-AS1#3: UAU CCG GUG AUG CUG AUG C. The three siRNAs were mixed together and used in our study, and however, si-VIM-AS1#1 was the best one for knocking down VIM-AS1 and si-VIM-AS1#1 was constructed into a lentivirus. Then, the miR-105-5p-related sequences were listed as below, anti-miR-105-5p, 5'-ACC ACA GGA CAC AGC AUU UGA-3', and miR-105-5p mimic, 5'-UCA AAU GCU CAG ACU CCU GUG GU-3'. Finally, the pmirGLO-VIM-AS1-WT or -Mut and pmirGLO-WEE1-3'UTR-WT (wild type) or -Mut (mutant), and pcDNA-VIM-AS1 were prepared by GenePharma (Shanghai, China).

CCK-8 Assays

In this study, we performed Cell Counting Kit-8 (CCK-8) assay (Sigma-Aldrich, Shanghai, China) to assess the cell viability of cancer cell lines (3×10^3 cells/well) in 96-well plates (Corning, Shanghai, China). The cells were firstly transfected with siRNAs or plasmids for 48 h. After transfection, the cell viability of glioma cells was examined at 450 nm for each well every 24 h using a microplate reader (Thermo Fisher Scientific, Waltham, MA, USA). All experiments were conducted in quadruplicate, and every assay was repeated three times. All the other agents were bought from Sigma-Aldrich (Shanghai, China).

Colony Formation Assay

The cancer cells were prepared into single-cell suspensions after 48 h transfection. Tumor cells were seeded into 6-well plates (HyClone, Logan, UT, USA) at a density of 3000 cells/well, and the media required to be replaced every three days. After 15 days, the visible colonies were captured and counted after methanol fixation and staining with 0.1% crystal violet (Sigma-Aldrich, Shanghai, China). Three wells for each treatment group were prepared, and every assay was independently repeated three times.

Flow Cytometry

To determine the cell apoptosis, the cancer cells were plated in 12-well plates. U87 and LN-229 cells were collected at 100 g for 5 min after 48 h transfection. Then, the resuspended cells were incubated with Annexin-V/fluorescein isothiocyanate (FITC) and propidium iodide (PI) kit (Sigma-Aldrich, Shanghai, China) in the dark for

15 min and 3 min, respectively. Finally, the cell apoptosis rate of U87 and LN-229 cells was detected on Bio-Rad S3e flow cytometry (Hercules, CA, USA). We set three wells for each treatment group, and every assay was independently repeated three times.

To analyze the cell cycle of glioma cells, the cancer cells were plated in 12-well plates. After 48 h transfection, the collected cells were fixed with 70% methanol at 4°C overnight. Next, these harvested cells were incubated with ribonuclease A at a 37°C-thermostat water bath (Thermo Fisher Scientific, Waltham, MA, USA) for half an hour. Finally, these cells were incubated with PI at the concentration of 100 ng/mL for 10 minutes to labeled nuclei in the dark. The cell cycle was measured on Bio-Rad S3e flow cytometry. All the used agents were from Sigma-Aldrich (Shanghai, China).

Quantitative Real Time-PCR

The RNA was extracted from cancer cells or clinical tissues using TRIzol reagent (Thermo Fisher Scientific, Waltham, MA, USA). Then, 1 µg RNA was reverse transcribed to obtain complementary DNA (cDNA) by applying PrimeScript RT Kit (TaKaRa, Dalian, Liao Ning, China). In this study, we applied SYBR Premix Ex Taq II (Perfect Real-Time, TaKaRa, Dalian, Liao Ning, China) to determine the expression of lncRNA, miRNA, or mRNA. The 18S RNA was used as an internal control of VIM-AS1, U6 was considered as an internal control of miR-105-5p, and glyceraldehyde-3-phosphate dehydrogenase (GAPDH) was used as an internal control of other mRNAs. The primers were listed below. Cyclin A1, Forward: 5'-ATA ACG ACG GGA AGA GCG GG-3', Reverse: 5'-CTC CAT CCC AAG TGA CGA GC-3'; Bcl-2, Forward: 5'-CTT TGA GTT CGG TGG GGT CA-3', Reverse: 5'-GGG CCG TAC AGT TCC ACA AA-3'; PCNA, Forward: 5'-CTC TTC CCT TAC GCA AGT CTC A-3', Reverse: 5'-GTC TAG CTG GTT TCG GCT TCA-3'; Bax, Forward: 5'-GGG TTG TCG CCC TTT TCT AC-3', Reverse: 5'-AGT CGC TTC AGT GAC TCG G-3'; WEE1, Forward: 5'-GCA CTT GTC TTT GAC TTG TGT T-3', Reverse: 5'-ATC AAA ATG TGC CCT CTG CTT T-3'; E-cadherin, Forward: 5'-GCT GGA CCG AGA GAG TTT CC-3', Reverse: 5'-CGA CGT TAG CCT CGT TCT CA-3'; N-cadherin, Forward: 5'-TGT GCA TGA AGG ACA GCC TC-3', Reverse: 5'-AGC TTC TCA CGG CAT ACA CC-3'; Vimentin, Forward: 5'-GCA CAT TCG AGC AAA GAC AGG-3', Re-

verse: 5'-AGG GCT CCT AGC GGT TTA GG-3'; GAPDH, Forward: 5'-CAC CCA CTC CTC CAC CTT TG-3', Reverse: 5'-CCA CCA CCC TGT TGC TGT AG-3'. VIM-AS1, Forward: 5'-CAA AGC TCC CTT TGG ATG AC-3', Reverse: 5'-ACT AGT ACA CCC CCG ACG TG-3'; 18S RNA, Forward: 5'-CGT TCT TAG TTG GTG GAG CG-3', Reverse: 5'-CCG GAC ATC TAA GGG CAT CA-3'. U6, reverse-transcription PCR primers, 5'-GTC GTA TCC AGT GCA GGG TCC GAG GTA TTC GCA CTG GAT ACC ACA-3'; real-time PCR, Forward: 5'-UCA AAU GCU CAG ACU C-3', Reverse: 5'-GTG CAG GGT CCG AGG T-3'. All these primers were synthesized by Sangon Biotech Co., Ltd. (Shanghai, China). The relative VIM-AS1, miR-105-5p, and WEE1 expression were calculated using the equation $2^{-\Delta\Delta Ct}$.

Transwell Assays

Glioma cell lines were transfected with siRNAs and plasmids for 72 h. Then, 1.5×10^5 cells per well of 24-well trans-well plates were placed into the up-chambers (Corning, Shanghai, China). Meanwhile, a 10% FBS-contained DMEM was added to the bottom chambers of multi-well plates. Post incubation overnight, the migrated cells (at the bottom) were stained with crystal violet, and then, they were captured and counted under $\times 400$ magnification. All transwell assays were conducted in quadruplicate and repeated triplicate.

Western Blot Analysis

The protein samples were prepared with protease inhibitor cocktail-contained radioimmunoprecipitation assay (RIPA) lysate (Beyotime, Shanghai, China). These samples were denatured for 15 min at 98°C. Then, 30-50 μ g of proteins were added on 8% sodium dodecyl sulfate (SDS)-polyacrylamide gel electrophoresis (SDS-PAGE; Bio-Rad, Hercules, CA, USA), and protein bands-contained gels were transferred to 0.22 μ m polyvinylidene difluoride (PVDF) membranes (Bio-Rad, Hercules, CA, USA) for half an hour using Trans-Blot[®] Turbo[™] Transfer System (Bio-Rad, Hercules, CA, USA). Next, the transferred PVDF membranes were incubated with 1% Bovine Serum Albumin (BSA) in phosphate-buffered saline (PBS), and the membranes were cov-

ered with primary antibody at 4°C for 8 h. In the following step, these PVDF membranes were coated with goat-anti-mouse or goat anti-rabbit secondary antibody, which was conjugated by horseradish peroxidase (HRP), for 1 hour diluted at 1: 50,000 (Bioworld Technology, Nanjing, Jiang Su, China). All the primary antibodies including anti-PCNA, anti-Cyclin A1, anti-E-cadherin, anti-N-cadherin, anti-Vimentin, anti-Bcl-2, anti-Bax, and anti-GAPDH were bought from Cell Signal Technology (CST, Danvers, MA, USA). All the other used materials and agents were from Sigma-Aldrich (Shanghai, China).

Dual-Luciferase Reporter Assays

Firstly, 5×10^4 cells per well were plated in 24-well plates. The cancer cells (U87 and LN-229) were co-transfected with pmirGLO-VIM-AS1-WT (wide type), pmirGLO-VIM-AS1-mut (mutant), or pmirGLO-WEE1-3'UTR WT or pmirGLO-WEE1-3' untranslated region (UTR)-mut reporter plasmids, and Mock (negative control), miR-105-5p mimics, and anti-miR-105-5p. Post 24 h transfection, we determined the Luciferase activity using the Dual-Luciferase Assay Kit on GloMax 20/20 Luminometer (Promega, Madison, WI, USA).

RNA Immunoprecipitation Assays

To detect the potential interaction of VIM-AS1 with miR-105-5p, we conducted RNA immunoprecipitation assays (RIP) using the Magna RIP RNA-binding protein immunoprecipitation kit (Millipore, Billerica, MA, USA). The prepared cell lysate was incubated with anti-Argonaute-2 (Ago2)-contained buffer, IgG was used as a negative control, and both anti-Ago2 and IgG were from Sigma-Aldrich (cat. no. # SAB4200085, Shanghai, China). Finally, the obtained immunoprecipitated RNA samples were analyzed by real-time PCR for examining VIM-AS1 and miR-105-5p content. All experiments were conducted in quadruplicate, and every assay was repeated for triplicates.

Animal Experiments

The U87 cells were incubated with viruses for 24 h. The indicated lentiviruses were from HanBio Biotechnology (Shanghai, China). These transfected U87 cells were harvested at 100 g \times 5 min, and 3×10^6 cells were inoculated into 5-week old BALB/c nude mice. The nude mice were from the Model Animal Research Center of Nanjing University (Nanjing, Jiang Su, China). The clinical processes were approved by the Ethics Com-

mittee of Shanghai Jiao Tong University. In the following days, tumor volume was calculated every three days, according to this formula: (length \times width 2)/2. On the 15th day after injection, Western blot analysis was conducted to determine the levels of anti-PCNA, anti-Cyclin A1, anti-E-cadherin, anti-N-cadherin, anti-Vimentin, anti-Bcl-2, anti-Bax, and anti-GAPDH (CST, Danvers, MA, USA) in tumors of nude mice.

Statistical Analysis

The data in this study were expressed as mean \pm standard deviation (SD). A *p*-value < 0.05 was statistically significant. The data were statistically analyzed using the Statistical Product and Service Solution software package (version 19.0, SPSS Corp., Armonk, NY, USA) and GraphPad Prism 6 (GraphPad Software, La Jolla, CA, USA). Statistical significance was tested by Two-tailed Student's *t*-test for two groups comparisons and One-way analysis of variance (ANOVA) test with post-hoc analysis contrasts for multi-groups comparisons.

Results

VIM-AS1 Indicated a Poor Survival of Glioma-Carried Patients and it Was Upregulated in Cancer Tissues

In this study, bioinformatics analysis showed that VIM-AS1 was associated with poor survival of patients (Figure 1A). Then, real-time PCR revealed that VIM-AS1 was upregulated in cancer tissues (Figure 1B-C).

Knockdown of VIM-AS1 Suppressed Glioma Cell Proliferation, Growth, and Migration In Vitro

To examine the role of VIM-AS1 in glioma progression, we inhibited VIM-AS1 expression in U87 and LN-229 cells. Real-time PCR analysis demonstrated that VIM-AS1 was increased in U87, LN-229, U251, and T98G cells (Figure 2A), and it can be knocked down by small interfering RNA (Figure 2B). Importantly, CCK-8 assay analysis proved that the suppression of VIM-AS1 significantly inhibited cell proliferation of U87 and LN-229 (Figure 2C). The results of colony formation assay silencing of VIM-AS1 also repressed glioma cell growth (Figure 2D-E). We observed that interfering VIM-AS1 also significantly arrested U87 and LN-229 in the G0/G1 cell phase (Figure 2F). Furthermore, the knockdown of VIM-AS1 may remarkably inhibit the expression of cell cycle-related gene, including Cyclin A1 and PCNA (Figure 2G). On the other hand, transwell assay analysis demonstrated that the knockdown of VIM-AS1 markedly suppressed migration of both U87 and LN-229 cells (Figure 2H-I). Moreover, the silencing of VIM-AS1 significantly inhibited expression of migration-associated genes including E-cadherin, N-cadherin, and Vimentin (Figure 2J).

Knockdown of VIM-AS1 Increased Glioma Apoptosis of U87 and LN-229 In Vitro

Next, flow cytometry analysis explored that the suppression of VIM-AS1 can significantly increase glioma cell apoptosis (Figure 3A-B). Further study showed that

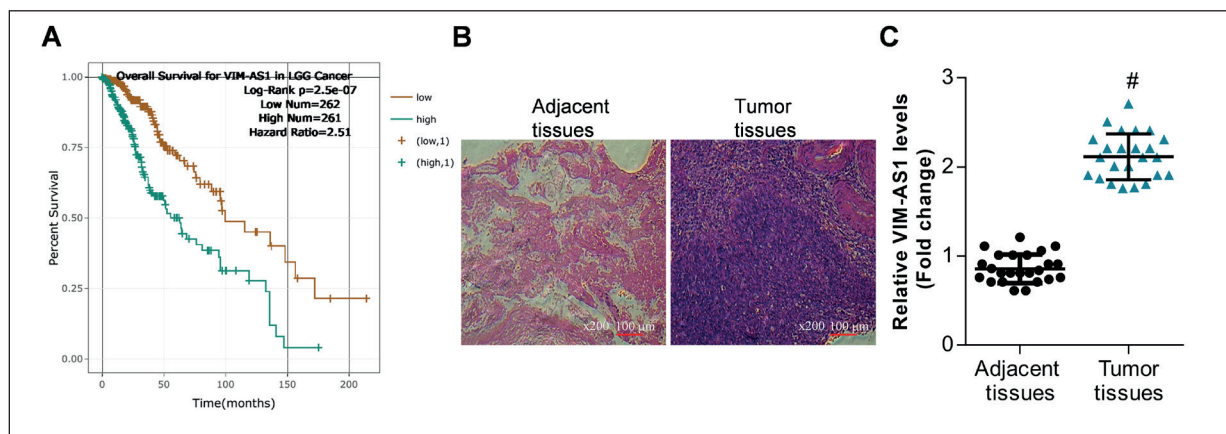


Figure 1. LncRNA VIM-AS1 was overexpressed in glioma tissues. **A**, The correlation of VIM-AS1 with the survival rate of glioma analyzed on STARBASE web. **B**, Histopathology of glioma determined by H&E analysis, and they were captured on a microscope (x200 magnifications). **C**, Real-time PCR analysis of VIM-AS1 expression in clinical samples, $\#p<0.01$, vs. adjacent tissues.

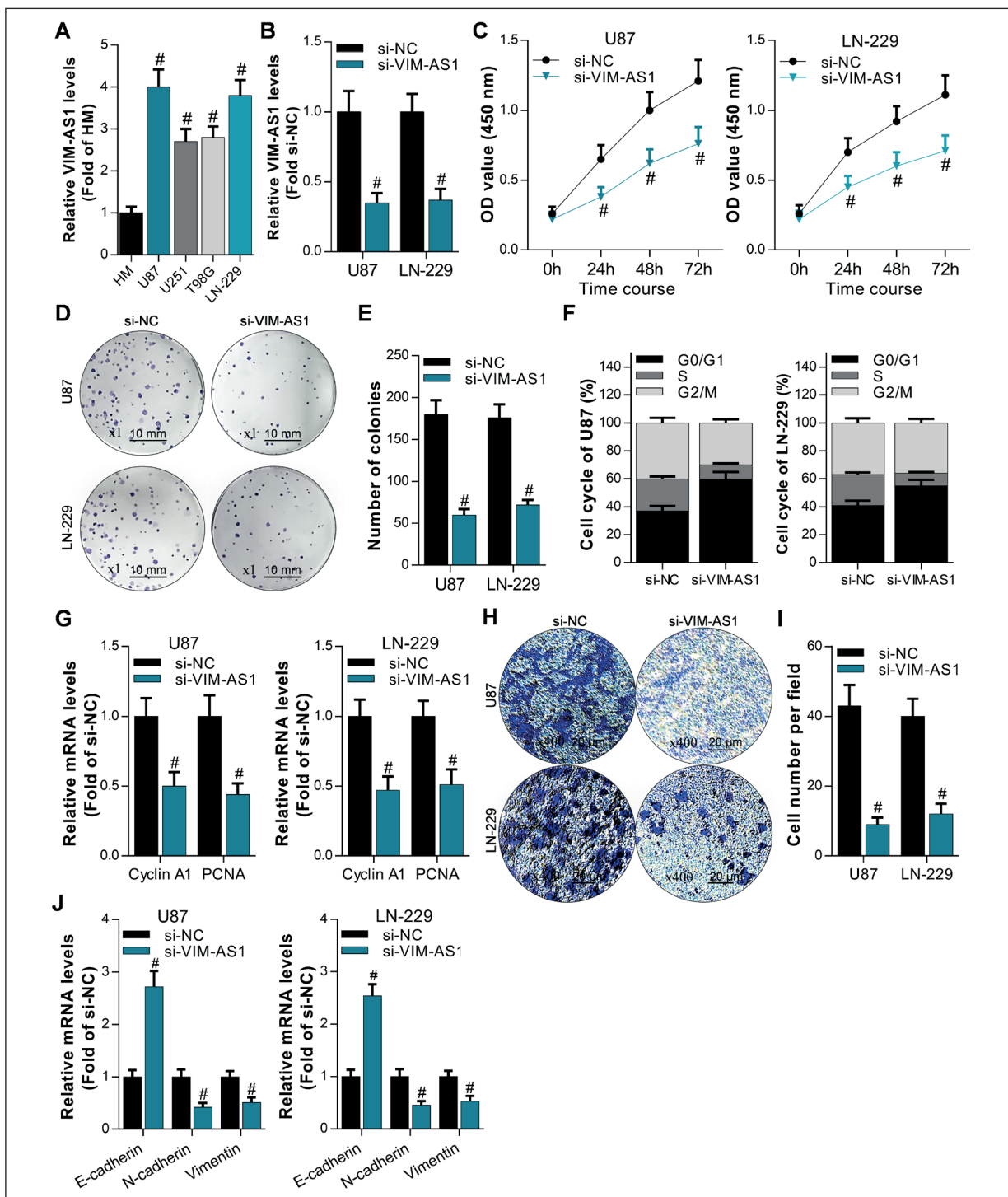


Figure 2. Knockdown of VIM-AS1 suppressed glioma cell proliferation and migration. **A**, Real Time-PCR analysis of VIM-AS1 in glioma cell lines, $^{\#}p<0.01$, vs. HM. **B**, Real-time PCR analysis of VIM-AS1 expression in U87 and LN-229 after 48 h transfection, $^{\#}p<0.01$, compared with si-NC. **C**, CCK-8 analysis of glioma cell proliferation at the indicated time after transfection, $^{\#}p<0.01$, compared with si-NC. **D-E**, Colony formation analysis of glioma cell growth after transfection and the colonies were captured ($\times 1$ magnifications) and statistically analyzed, $^{\#}p<0.01$ vs. si-NC. **F**, Flow cytometry analysis of cell cycle of U87 and LN-229 after 72 h transfection, $^{\#}p<0.01$ compared with si-NC. **G**, Real-time PCR analysis of expression of cell cycle-related genes including Cyclin A1 and PCNA, after 72 h transfection, $^{\#}p<0.01$ compared with si-NC. **H-I**, Trans-well assay analysis of glioma cell migration after transfection and the migrated cells were captured ($\times 400$ magnifications) and statistically analyzed, $^{\#}p<0.01$ compared with si-NC. **J**, Real-time PCR analysis of expression of cell migration-related genes including E-cadherin, N-cadherin, and Vimentin after 72 h transfection, $^{\#}p<0.01$ vs. si-NC.

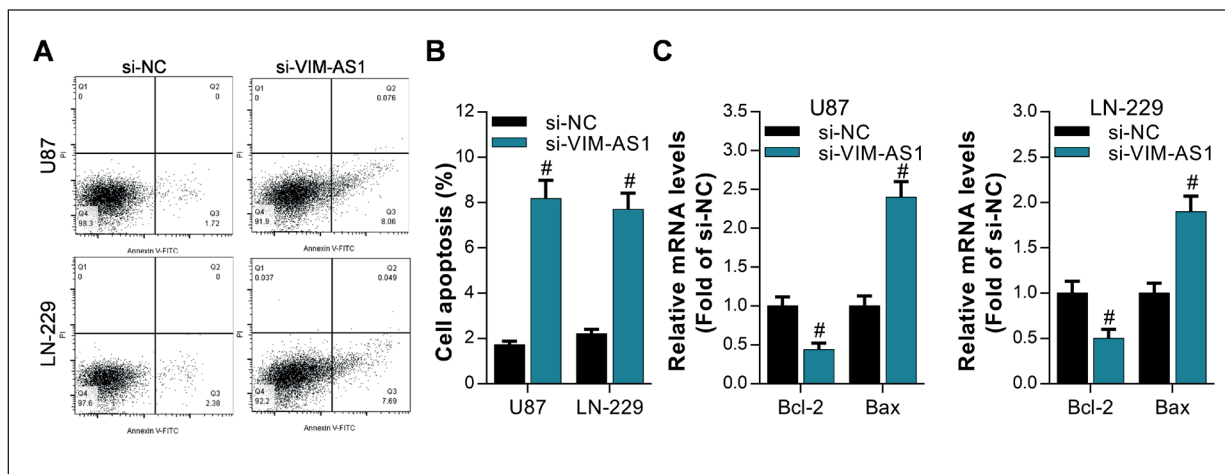


Figure 3. Knockdown of VIM-AS1 increased glioma cell apoptosis. **A-B**, Annexin V-FITC/PI staining analysis of the glioma cell apoptosis rate after 72 h transfection in U87 and LN-229 cells, and the apoptosis rate was statistically analyzed, * $p<0.01$ vs. si-NC. **C**, Real-time PCR analysis of expression of the cell apoptosis-related genes including Bcl-2 and Bax after 72 h transfection, * $p<0.01$ vs. si-NC.

the silencing of VIM-AS1 markedly downregulated Bcl-2 expression, while the knockdown of VIM-AS1 upregulated Bax levels (Figure 3C).

Knockdown of VIM-AS1 Inhibited Tumor Growth In Vivo

To investigate the role of VIM-AS1 in glioma progression *in vivo*, the nude mice were used in this study, and we constructed lentiviruses used for knocking down the expression of VIM-AS1 in U87 cells. In the beginning, U87 glioma cells were incubated with these lentiviruses for 30 h. These treated cells were implanted into 5-week old BALB/c nude mice. Then, the tumor volume was measured every three days (Figure 4A). The data revealed that the downregulation of VIM-AS1 significantly decreased the tumor volume and tumor weight (Figure 4A-C). Consistently, the suppression of VIM-AS1 significantly depressed the expression of Cyclin A1, PCNA, N-cadherin, Vimentin, and Bcl-2, while the suppression of VIM-AS1 elevated the expression of E-cadherin and Bax in these xenografts (Figure 4D-E).

Reciprocal Suppression Between VIM-AS1 and MiR-105-5p in Glioma Cells

To explore the molecular mechanism of VIM-AS1 in glioma development, we examined the relationship of VIM-AS1 with miR-105-5p. Firstly, the bioinformatic data showed that the expression of VIM-AS1 was negatively correlated with miR-105-5p in glioma tissues (Figure 5A). Secondly, we observed that the high expression of miR-105-5p indicated a better survival of patients (Figure 5B).

Furthermore, the GEO microarray records and real-time PCR analysis evidenced that miR-105-5p was significantly reduced in tumor tissues (Figure 5C-D). Then, the overexpression of miR-105-5p significantly decreased the Luciferase activity of pGLO-VIM-AS1 in U87 and LN-229 cells, while it failed to affect the Luciferase activity of pGLO-VIM-AS1-Mut which carried mutated binding sites (Figure 5E-F). Moreover, real-time PCR assays demonstrated that the overexpression of miR-105-5p significantly downregulated the VIM-AS1 expression in U87 and LN-229 cells (Figure 5G). Finally, RNA immunoprecipitation assay revealed that both miR-105-5p and VIM-AS1 were able to bind with Ago2 protein (Figure 5H-I).

VIM-AS1 Blocked the Cancer-Suppressing Role of MiR-105-5p

To determine the function of reciprocal suppression between VIM-AS1 and miR-105-5p in glioma development, we overexpressed miR-105-5p and VIM-AS1 in both U87 and LN-229 cells (Figure 6A). The data of CCK-8 assay showed that the overexpression of miR-105-5p can inhibit the glioma cell proliferation, and however, miR-105-5p-mediated inhibition can be blocked by the overexpression of VIM-AS1 (Figure 6B). Similarly, VIM-AS1 also significantly abolished miR-105-5p-mediated suppression of glioma cell colony formation (Figure 6C). Then, we observed that the overexpression of miR-105-5p markedly arrested glioma cells in the G0/G1 phase, and however, these changes of cell cycles were reversed by overexpression of VIM-AS1 (Figure 6D). Consis-

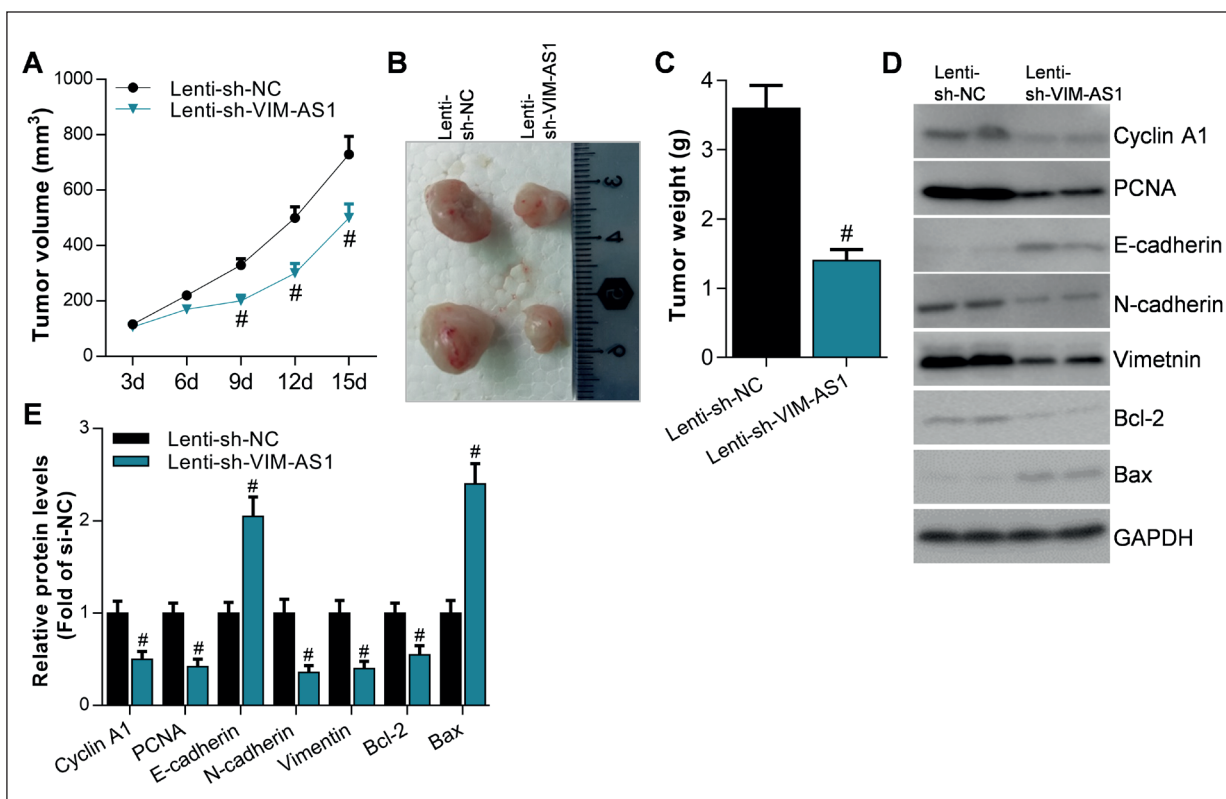


Figure 4. Knockdown of VIM-AS1 repressed tumor growth *in vivo*. **A**, The volume of tumors at the indicated time after implantation, * $p<0.01$ vs. lenti-NC. **B**, The tumors were captured on the 15th day. **C**, The weight of tumors on the 15th day after implantation, * $p<0.01$ compared with lenti-NC. **D-E**, Western blot analysis of gene expression in tumors, and Image J software analysis of the corresponding optical density of protein bands, * $p<0.01$ vs. lenti-NC.

tently, the overexpression of VIM-AS1 blocked the overexpression of miR-105-5p-induced decrease of Cyclin A1 and PCNA (Figure 6E).

Next, VIM-AS1 significantly attenuated miR-105-5p-induced apoptosis and migration of both U87 and LN-229 cells evidenced by annexin V-FITC/PI staining and transwell assay (Figure 6F, H). Furthermore, the overexpression of VIM-AS1 neutralized overexpression of miR-105-5p-mediated regulation of Bcl-2, Bax, and E-cadherin, N-cadherin, and Vimentin (Figure 6G, I).

Oncogene WEE1 Was Synergistically Controlled by VIM-AS1 and MiR-105-5p

To examine the downstream target of miR-105-5p, bioinformatic analysis exhibited that expression of VIM-AS1 was positively correlated with the expression of WEE1, and the expression of miR-105-5p was negatively correlated with the expression of WEE1 (Figure 7A). Then, the binding of miR-105-5p on WEE1 3'UTR was predicted on the STARBASE web (Figure 7B). The Luciferase reporter assays proved that miR-105-5p significant-

ly inhibited Luciferase activity of pGLO-WEE1-3'UTR, which was activated by VIM-AS1 in U87 and LN-229 cells (Figure 7C-D). Interestingly, the Luciferase activity of pGLO-WEE1-3'UTR was synergistically controlled by VIM-AS1 and miR-105-5p (Figure 7C-D). VIM-AS1 can abolish miR-105-5p-mediated downregulation of Luciferase activity, and meanwhile, miR-105-5p can block VIM-AS1-induced upregulation of Luciferase activity (Figure 7C-D). Consistently, the overexpression of miR-105-5p markedly decreased WEE1 expression, and the overexpression of VIM-AS1 increased WEE1 expression at mRNA and protein levels (Figure 7E-G). More importantly, we observed that the expression of oncogene WEE1 was synergistically modulated by VIM-AS1 and miR-105-5p (Figure 7E-G).

Discussion

Glioma, especially glioblastoma, is one of the main cause of brain cancer-induced death in Chi-

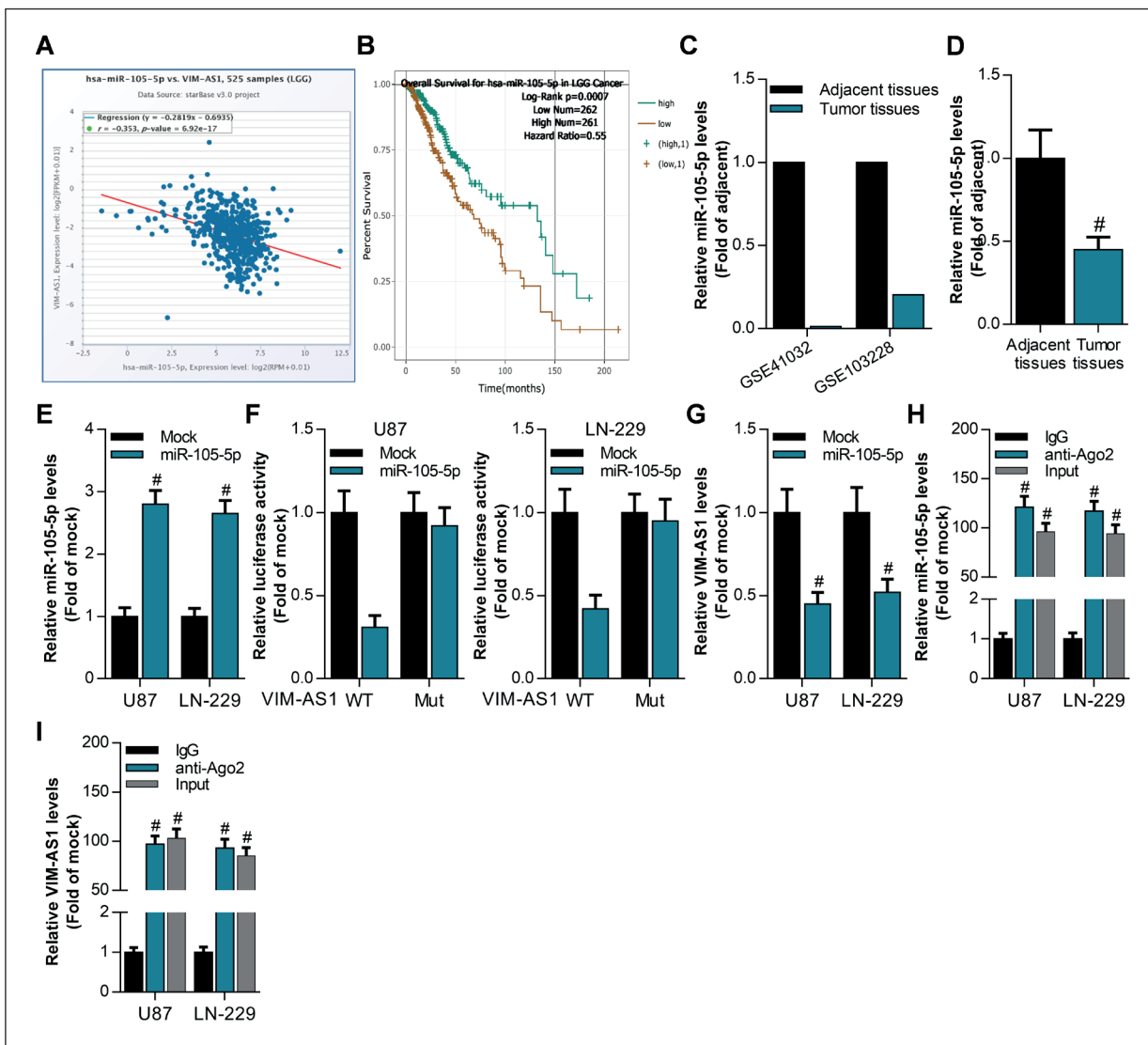


Figure 5. Reciprocal inhibition between VIM-AS1 and miR-105-5p in glioma cells. **A**, The correlation of VIM-AS1 with miR-105-5p analyzed on the STARBASE web. **B**, The correlation of miR-105-5p with survival rate of glioma analyzed on STARBASE web. **C**, The expression of miR-105-5p in microarray GSE41032 and GSE103228. **D**, Real-time PCR analysis of miR-105-5p in clinical tumor tissues and adjacent tissues, $^{\#}p < 0.01$ vs. adjacent tissues. **E**, Real-time PCR analysis of miR-105-5p expression after 72 h transfection in U87 and LN-229 cells, $^{\#}p < 0.01$ vs. Mock. **F**, Luciferase reporter assay analysis of pGLO-VIM-AS1 after 72 h transfection with miR-105-5p, $^{\#}p < 0.01$ vs. Mock. **G**, Real-time PCR analysis of VIM-AS1 expression after 72 h transfection with miR-105-5p in glioma cells, $^{\#}p < 0.01$ compared with Mock. **H-I**, Real-time PCR analysis of miR-105-5p and VIM-AS1 content after performing the RNA immunoprecipitation assay with anti Ago2 in U87 and LN-229 cells, $^{\#}p < 0.01$ compared with IgG.

na as well, as in Europe and the United States¹⁻³. Many reports have explored that many lncRNAs are involved in human diseases, including gliomas. For instance, HOTAIR¹⁴, NEAT1¹⁵, TP73-AS1¹⁶, CRNDE¹⁷, H19¹⁸, SOX2OT¹⁰, XIST¹⁹, GAS5²⁰, and MALAT1²¹ are participating in glioma progression through diverse molecular mechanisms. In previous studies, VIM-AS1 can function as an oncogene in colorectal cancer *via* inducing EMT²³, and addition-

ally, VIM-AS1 also can positively regulate Vimentin expression²². In accordance with previous studies, we firstly verified the oncogenic role of VIM-AS1 and identified VIM-AS1 as a potential prognostic indicator in patients with glioma in this study. By conducting *in vitro* and *in vivo* experiments, we confirmed that VIM-AS1 could act as a sponge of miR-105-5p, which may decrease WEE1 expression by targeting 3'UTR of WEE1. Knockdown

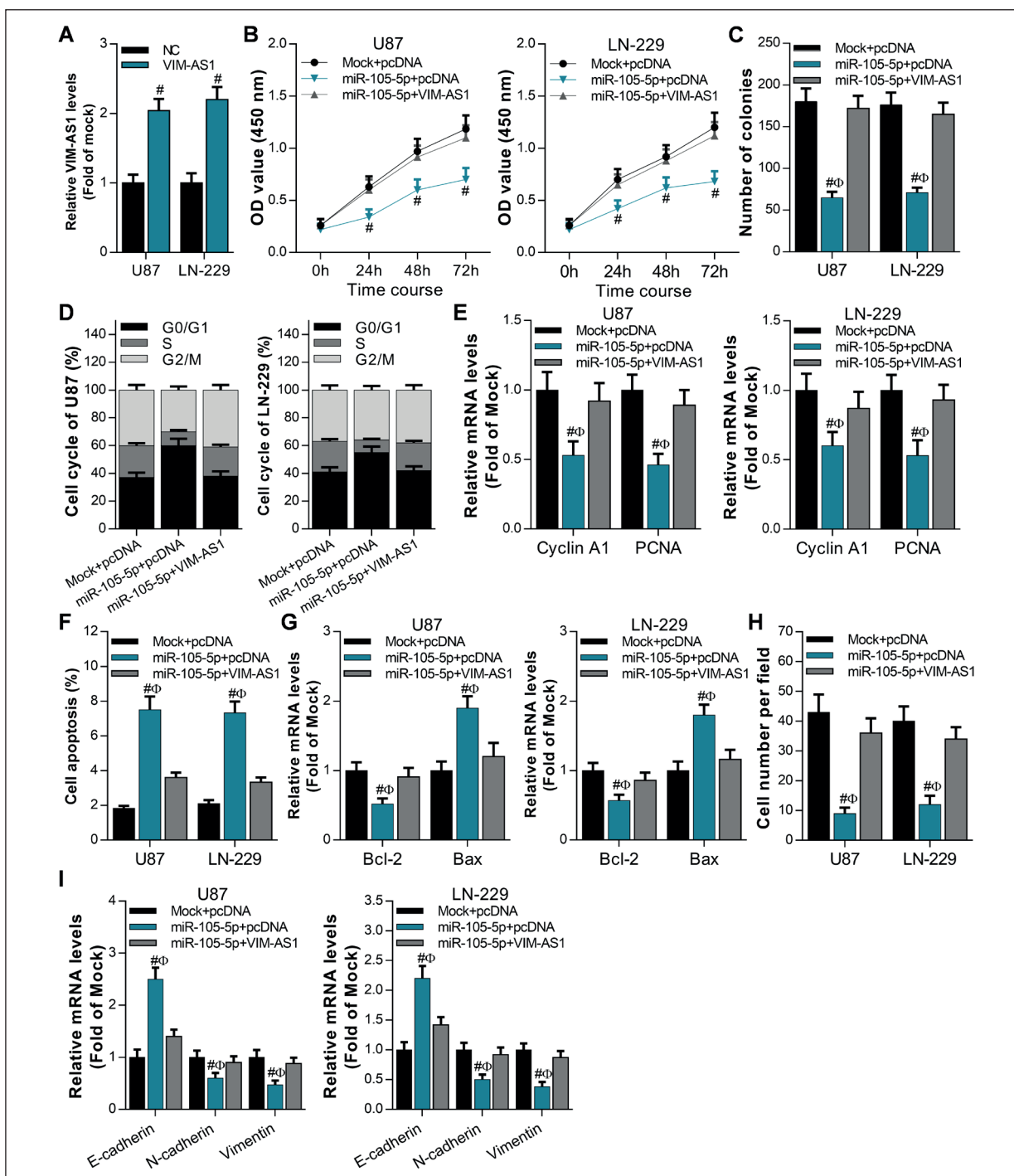


Figure 6. VIM-AS1 attenuated the cancer-suppressing role of miR-105-5p. **A**, Real-time PCR analysis of VIM-AS1 after 72 h transfection in U87 and LN-229 cells, * $p<0.01$ vs. Mock+pcDNA. **B**, CCK-8 analysis of glioma cell proliferation at the indicated time after transfection, * $p<0.01$, vs. Mock+pcDNA. **C**, Colony formation analysis of glioma cell growth after transfection and the colonies were captured and statistically analyzed, * $p<0.01$ vs. Mock+pcDNA. **D**, Flow cytometry analysis of cell cycle of U87 and LN-229 after 72 h transfection. **E**, Real-time PCR analysis of expression of cell cycle-related genes including Cyclin A1 and PCNA, after 72 h transfection, * $p<0.01$ vs. Mock+pcDNA. **F**, Annexin V-FITC/PI staining analysis of glioma the cell apoptosis rate after 72 h transfection in U87 and L-229 cells, and the apoptosis rate was statistically verified, * $p<0.01$ vs. Mock+pcDNA. **G**, Real-time PCR analysis of expression of the cell apoptosis-related genes including Bcl-2 and Bax after 72 h transfection, * $p<0.01$ vs. Mock+pcDNA. **H**, Transwell assay analysis of glioma cell migration after transfection and the migrated cells were captured and statistically evaluated, * $p<0.01$ vs. Mock+pcDNA. **I**, Real-time PCR analysis of expression of cell migration-related genes including E-cadherin, N-cadherin, and Vimentin after 72 h transfection, * $p<0.01$ vs. Mock+pcDNA.

of VIM-AS1 depressed glioma cell proliferation, migration, and increased the cell apoptosis *in vitro* and *in vivo*, implying that downregulation of VIM-AS1 could be a beneficial treatment in glioma patients. Consequently, inhibition of VIM-AS1 could improve glioma progression.

LncRNAs always modulate behaviors of cancer cells by regulating the expression of oncogenes and expression of tumor suppressors by functioning as sponges for lots of miRNAs

resulting in suppressing miRNAs-mediated effects on its downstream target mRNAs^{10,13-21}. In our study, bioinformatics analysis exhibited that VIM-AS1 can directly bind with miR-105-5p. Luciferase reporter assays demonstrated that miR-105-5p overexpression significantly repressed Luciferase activity of pGLO-VIM-AS1, indicating that VIM-AS1 possessed miR-105-5p binding site. In accordance with the data of Luciferase assays, the overexpression of miR-105-

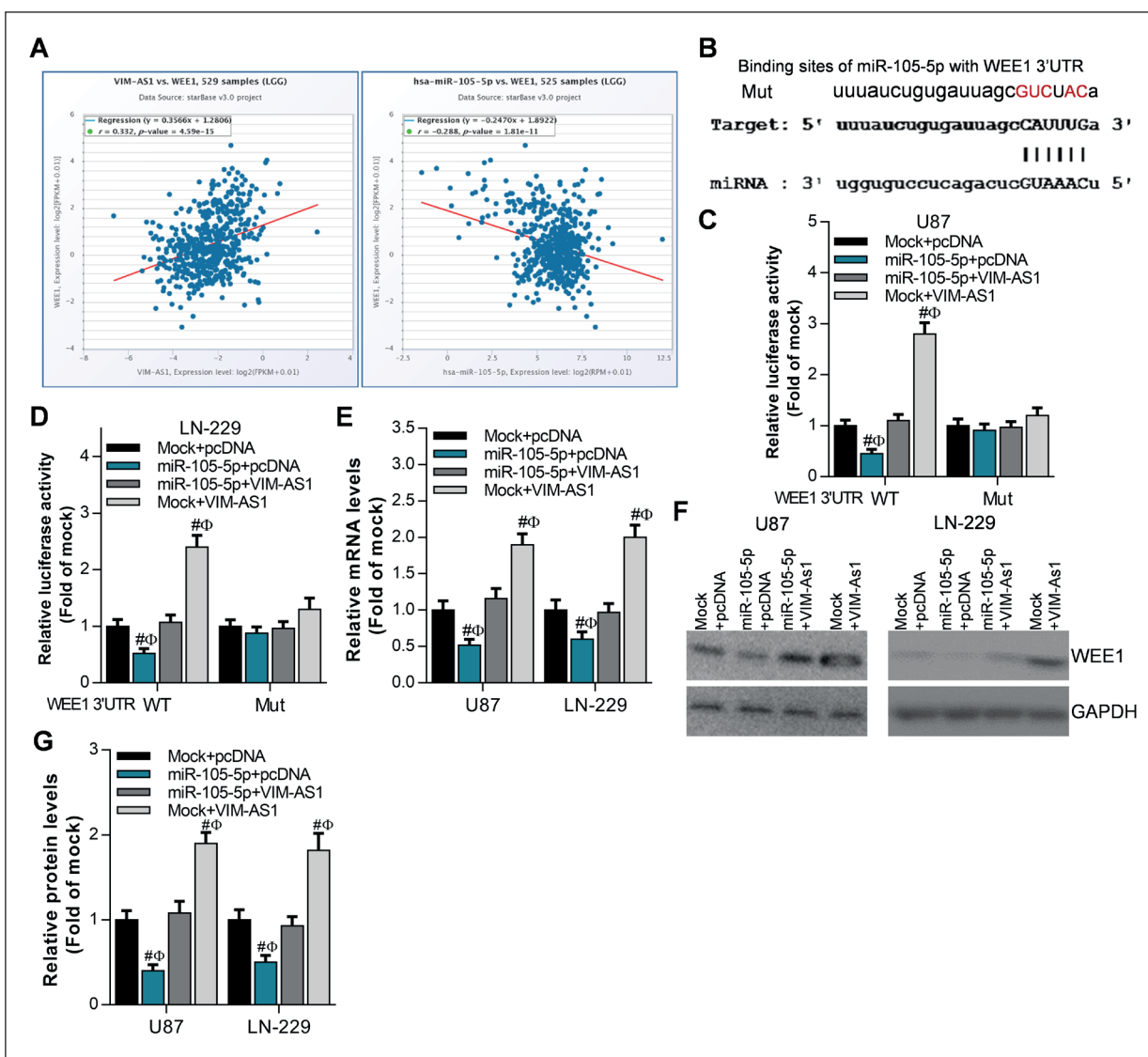


Figure 7. Tumor enhancer WEE1 was synergistically controlled by VIM-AS1 and miR-105-5p. **A**, The correlation of VIM-AS1 and miR-105-5p with WEE1 respectively analyzed on STARBASE web. **B**, The schematic of predicted binding sites of miR-105-5p with WEE1 sequence on STARBASE web. **C-D**, Luciferase reporter assay analysis of pGLO-WEE1-3'UTR after 72 h transfection with the indicated nucleotide sequence and plasmids, ${}^{\#}p < 0.01$ compared with Mock+pcDNA. **E**, Real-time PCR analysis of WEE1 after 72 h transfection with the indicated nucleotide fragment, ${}^{\#}p < 0.01$ vs. Mock+pcDNA. **F-G**, Western blot analysis of WEE1 after 72 h transfection, and Image J software analysis of the corresponding optical density of protein bands, ${}^{\#}p < 0.01$ vs. Mock+pcDNA.

5p significantly inhibited VIM-AS1 levels in glioma cells. More importantly, an endogenous interaction was observed between VIM-AS1 and miR-105-5p using anti-Ago2 antibody, and reciprocal suppression was observed between VIM-AS1 and miR-105-5p in glioma cells. In the previous study, miR-105-5p was reported as a tumor suppressor by targeting SOX9²⁴, and meanwhile, it was a negative regulator for metastasis of triple-negative breast cancer²⁵. Consistently, miR-105-5p significantly decreased colony formation, proliferation, and migration of both U87 and LN-229 cells, and miR-105-5p also markedly enhanced the cell apoptosis of glioma cell lines *in vitro*, while miR-105-5p-controlled these glioma cell behaviors can be partly abolished by overexpression of VIM-AS1. Thus, VIM-AS1 exerted oncogenic functions on human glioma by downregulating miR-105-5p expression.

MiRNAs often present its functions by binding 3'UTR of downstream targets. In this study, miR-105-5p could significantly inhibit the expression of its target gene WEE1. WEE1 is an oncogene involved in cancer cell proliferation, apoptosis, and invasion²⁶⁻²⁸, and nowadays, chemical inhibitors, such as AZD-1775 and MK-1775, have been developed to target WEE1 resulting in improvement of WEE1-associated cancers²⁹⁻³³, suggesting that WEE1 is a meaningful target for cancer treatment. Therefore, miR-105-5p could exert its anti-cancer activity by downregulating WEE1 expression in gliomas, implying that WEE1 was needed for miR-105-5p-regulated cell growth, migration, and apoptosis in glioma cells. Furthermore, VIM-AS1 could positively regulate WEE1 expression by sponging miR-105-5p in glioma cells evidenced by Luciferase reporter assay, real-time PCR, and Western blot, indicating that WEE1 is involved in VIM-AS1/miR-105-5p axis-mediated cancer progression. Finally, WEE1 was synergistically controlled by VIM-AS1 and miR-105-5p. Consequently, these findings revealed that VIM-AS1 could promote cell growth, migration, and it could inhibit the cell apoptosis *via* VIM-AS1/miR-105-5p/WEE1 axis in glioma progression.

Conclusion

In this study, VIM-AS1 was upregulated in glioma cancer tissues, and its high expression was positively associated with patients' worse prognosis. The knockdown of VIM-AS1 significantly inhibited cancer cell proliferation, migration,

while it increased cancer cell apoptosis of U87 and LN-229 cells. Thus, VIM-AS1 was an oncogene of glioma. Importantly, reciprocal repression between VIM-AS1 and miR-105-5p was observed in cancer cells, and the knockdown of VIM-AS1 reversed silencing of miR-105-5p-mediated glioma cell growth, migration, and apoptosis *in vitro*. Additionally, WEE1 was synergistically regulated by VIM-AS1 and miR-105-5p in both U87 and LN-229 cells. Moreover, WEE1-involved VIM-AS1/miR-105-5p axis was the essential mechanism of glioma progression by modulating cancer cell proliferation, migration, and apoptosis. Together, the knockdown of VIM-AS1 or WEE1, overexpression of miR-105-5p might inhibit glioma progression.

Acknowledgments

We thank our team for technical cooperation.

Funding

This study received no financial supporting from government subjects.

Ethical Approval

All applicable international, national, and/or institutional guidelines for the care and use of animals were followed. All procedures performed in our studies involving human participants were in accordance with the ethical standards of the Institutional and/or National Research Committee and with the 1964 Helsinki declaration and its later amendments or comparable ethical standards.

Informed Consent

Informed consent was obtained from all included participants.

Author Contributions

G.Y.T. designed the project. S.S.T., G.P., P.X.J., and N.D. performed the animal experiments, and they also cultured the cell lines and conducted the cell experiments. G.Y.T. and S.S.T. analyzed the experimental data. G.Y.T. offered discussion and suggestions. G.Y.T. and S.S.T. wrote the manuscript. G.Y.T. provided the financial support. All authors reviewed the manuscript.

Conflict of Interests

All authors declare no competing financial interests.

References

- 1) PORTER KR, MCCARTHY BJ, FREELS S, KIM Y, DAVIS FG. Prevalence estimates for primary brain tumors in the United States by age, gender, behavior, and histology. *Neuro Oncol* 2010; 12: 520-527.
- 2) JIANG T, TANG GF, LIN Y, PENG XX, ZHANG X, ZHAI XW, PENG X, YANG JQ, HUANG HE, WU NF, CHEN XJ, XING HX, SU TY, WANG ZC. Prevalence estimates for primary brain tumors in China: a multi-center cross-sectional study. *Chin Med J* 2011; 124: 2578-2583.
- 3) OSTROM QT, GITTLEMAN H, XU J, KROMER C, WOLINSKY Y, KRUCHKO C, BARNHOLTZ-SLOAN JS. CBTRUS statistical report: primary brain and other central nervous system tumors diagnosed in the United States in 2009-2013. *Neuro Oncol* 2016; 18: v1-v75.
- 4) TANAKA S, LOUIS DN, CURRY WT, BATCHELOR TT, DIETRICH J. Diagnostic and therapeutic avenues for glioblastoma: no longer a dead end? *Nat Rev Clin Oncol* 2013; 10: 14-26.
- 5) MEYER MA. Malignant gliomas in adults. *N Engl J Med* 2008; 359: 1850-1850.
- 6) VEHLOW A, CORDES N. Invasion as target for therapy of glioblastoma multiforme. *Biochim Biophys Acta* 2013; 1836: 236-244.
- 7) ZHANG M, ZHAO K, XU X, YANG Y, YAN S, WEI P, LIU H, XU J, XIAO F, ZHOU H, YANG X, HUANG N, LIU J, HE K, XIE K, ZHANG G, HUANG S, ZHANG N. A peptide encoded by circular form of LINC-PINT suppresses oncogenic transcriptional elongation in glioblastoma. *Nat Commun* 2018; 9: 4475-4492.
- 8) YE J, ZHU J, CHEN H, QIAN J, ZHANG L, WAN Z, CHEN F, SUN S, LI W, LUO C. A novel lncRNA-LINC01116 regulates tumorigenesis of glioma by targeting VEGFA. *Int J Cancer* 2019; 29: 00-00.
- 9) LI Q, DONG C, CUI J, WANG Y, HONG X. Over-expressed lncRNA HOTAIRM1 promotes tumor growth and invasion through up-regulating HOXA1 and sequestering G9a/EZH2/Dnmts away from the HOXA1 gene in glioblastoma multiforme. *J Exp Clin Cancer Res* 2018; 37: 265.
- 10) SU R, CAO S, MA J, LIU Y, LIU X, ZHENG J, CHEN J, LIU L, CAI H, LI Z, ZHAO L, HE Q, XUE Y. Knockdown of SOX2OT inhibits the malignant biological behaviors of glioblastoma stem cells via up-regulating the expression of miR-194-5p and miR-122. *Mol Cancer* 2017; 16: 171-196.
- 11) WU W, YU T, WU Y, TIAN W, ZHANG J, WANG Y. The miR155HG/miR-185/ANXA2 loop contributes to glioblastoma growth and progression. *J Exp Clin Cancer Res* 2019; 38: 133.
- 12) BARTONICEK N, MAAG JL, DINGER ME. Long noncoding RNAs in cancer: mechanisms of action and technological advancements. *Mol Cancer* 2016; 15: 43.
- 13) KALLEN AN, ZHOU XB, XU J, QIAO C, MA J, YAN L, LU L, LIU C, YI JS, ZHANG H, MIN W, BENNETT AM, GREGORY RI, DING Y, HUANG Y. The imprinted H19 lncRNA antagonizes let-7 microRNAs. *Mol Cell* 2013; 52: 101-112.
- 14) KE J, YAO YL, ZHENG J, WANG P, LIU YH, MA J, LI Z, LIU XB, LI ZQ, WANG ZH, XUE YX. Knockdown of long non-coding RNA HOTAIR inhibits malignant biological behaviors of human glioma cells via modulation of miR-326. *Oncotarget* 2015; 6: 21934-21949.
- 15) ZHOU K, ZHANG C, YAO H, ZHANG X, ZHOU Y, CHE Y, HUANG Y. Knockdown of long non-coding RNA NEAT1 inhibits glioma cell migration and invasion via modulation of SOX2 targeted by miR-132. *Mol Cancer* 2018; 17: 105.
- 16) ZHANG R, JIN H, LOU F. The long non-coding RNA TP73-AS1 interacted with miR-142 to modulate brain glioma growth through HMGB1/RAGE pathway. *J Cell Biochem* 2018; 119: 3007-3016.
- 17) ZHENG J, LIU X, WANG P, XUE Y, MA J, QU C, LIU Y. CRNDE promotes malignant progression of glioma by attenuating miR-384/PIWI4/STAT3 axis. *Mol Ther* 2016; 24: 1199-1215.
- 18) JIA P, CAI H, LIU X, CHEN J, MA J, WANG P, LIU Y, ZHENG J, XUE Y. Long non-coding RNA H19 regulates glioma angiogenesis and the biological behavior of glioma-associated endothelial cells by inhibiting microRNA-29a. *Cancer Lett* 2016; 381: 359-369.
- 19) CHENG Z, LI Z, MA K, LI X, TIAN N, DUAN J, XIAO X, WANG Y. Long non-coding RNA XIST promotes glioma tumorigenicity and angiogenesis by acting as a molecular sponge of miR-429. *J Cancer* 2017; 8: 4106-4116.
- 20) ZHAO X, LIU Y, ZHENG J, LIU X, CHEN J, LIU L, WANG P, XUE Y. GAS5 suppresses malignancy of human glioma stem cells via a miR-196a-5p/FOXP1 feedback loop. *Biochim Biophys Acta Mol Cell Res* 2017; 1864: 1605-1617.
- 21) CAO S, WANG Y, LI J, LV M, NIU H, TIAN Y. Tumor-suppressive function of long noncoding RNA MALAT1 in glioma cells by suppressing miR-155 expression and activating FBXW7 function. *Am J Cancer Res* 2016; 6: 2561-2574.
- 22) BOQUE-SASTRE R, SOLER M, OLIVEIRA-MATEOS C, PORTELA A, MOUTINHO C, SAYOLS S, VILLANUEVA A, ESTELLER M, GUILL S. Head-to-head antisense transcription and R-loop formation promotes transcriptional activation. *Proc Natl Acad Sci USA* 2015; 112: 5785-5790.
- 23) REZANEJAD BARDAJI H, ASADI MH, YAGHOobi MM. Long noncoding RNA VIM-AS1 promotes colorectal cancer progression and metastasis by inducing EMT. *Eur J Cell Biol* 2018; 97: 279-288.
- 24) LIU X, WANG H, ZHU Z, YE Y, MAO H, ZHANG S. MicroRNA-105 targets SOX9 and inhibits human glioma cell progression. *FEBS Lett* 2016; 590: 4329-4342.
- 25) LI HY, LIANG JL, KUO YL, LEE HH, CALKINS MJ, CHANG HT, LIN FC, CHEN YC, HSU TI, HSIAO M, GER LP, LU PJ. miR-105/93-3p promotes chemoresistance and circulating miR-105/93-3p acts as a diagnostic biomarker for triple negative breast cancer. *Breast Cancer Res* 2017; 19: 133.
- 26) LEE JW, PARAMESWARAN J, SANDOVAL-SCHAEFER T, EOHN KJ, YANG DH, ZHU F, MEHRA R, SHARMA R, GAFFNEY SG, PERRY EB, TOWNSEND JP, SEREBRIISKII IG, GOLEMIS EA, ISSAEVA N, YARBROUGH WG, KOO JS, BURTNESS B. Combined Aurora Kinase A (AURKA) and WEE1

- inhibition demonstrates synergistic antitumor effect in squamous cell carcinoma of the head and Neck. *Clin Cancer Res* 2019; 25: 3430-3442.
- 27) BUKHARI AB, LEWIS CW, PEARCE JJ, LUONG D, CHAN GK, GAMPER AM. Inhibiting Wee1 and ATR kinases produces tumor-selective synthetic lethality and suppresses metastasis. *J Clin Invest* 2019; 129: 1329-1344.
 - 28) WU S, WANG S, GAO F, LI L, ZHENG S, YUNG WKA, KOUL D. Activation of WEE1 confers resistance to PI3K inhibition in glioblastoma. *Neuro Oncol* 2018; 20: 78-91.
 - 29) CHEN X, LOW KH, ALEXANDER A, JIANG Y, KARAKAS C, HESS KR, CAREY JPW, BUI TN, VIJAYARAGHAVAN S, EVANS KW, YI M, ELLIS DC, CHEUNG KL, ELLIS IO, FU S, MERIC-BERNSTAM F, HUNT KK, KEYOMARSI K. Cyclin E overexpression sensitizes triple-negative breast cancer to wee1 kinase inhibition. *Clin Cancer Res* 2018; 24: 6594-6610.
 - 30) GHELLI LUSERNA DI RORA A, BEEHARRY N, IMBROGNO E, FERRARI A, ROBUSTELLI V, RIGHI S, SABATTINI E, VERGA FALZACAPPA MV, RONCHINI C, TESTONI N, BALDAZZI C, PAPAYANNIDIS C, ABBENANTE MC, MARCONI G, PAOLINI S, PARISI S, SARTOR C, FONTANA MC, DE MATTEIS S, IACOBUCCI I, PELICCI PG, CAVO M, YEN TJ, MARTINELLI G. Targeting WEE1 to enhance conventional therapies for acute lymphoblastic leukemia. *J Hematol Oncol* 2018; 11: 99.
 - 31) LIN X, CHEN D, ZHANG C, ZHANG X, LI Z, DONG B, GAO J, SHEN L. Augmented antitumor activity by olaparib plus AZD1775 in gastric cancer through disrupting DNA damage repair pathways and DNA damage checkpoint. *J Exp Clin Cancer Res* 2018; 37: 129.
 - 32) MATHESON CJ, VENKATARAMAN S, AMANI V, HARRIS PS, BACKOS DS, DONSON AM, WEMPE MF, FOREMAN NK, VIBHAKAR R, REIGAN P. A WEE1 inhibitor analog of AZD1775 maintains synergy with cisplatin and demonstrates reduced single-Agent cytotoxicity in medulloblastoma cells. *ACS Chem Biol* 2016; 11: 2066-2067.
 - 33) POKORNY JL, CALLIGARIS D, GUPTA SK, IYEKEGBE DO, JR., MUELLER D, BAKKEN KK, CARLSON BL, SCHROEDER MA, EVANS DL, LOU Z, DECKER PA, ECKEL-PASSOW JE, PUCCI V, MA B, SHUMWAY SD, ELMQUIST WF, AGAR NY, SARKARIA JN. The efficacy of the Wee1 inhibitor mk-1775 combined with temozolomide is limited by heterogeneous distribution across the blood-brain barrier in glioblastoma. *Clin Cancer Res* 2015; 21: 1916-1924.